Effectiveness of Fixed-Bed Regenerators for Energy Recovery in Buildings Applications

Hadi Ramin[*], *Easwaran N. Krishnan*, and Carey J. Simonson

Department of Mechanical Engineering, University of Saskatchewan, Saskatoon, Canada

Abstract. Energy consumption for ventilation purposes in buildings makes up a considerable portion of HVAC energy consumption. Energy recovery ventilators (ERVs) can reduce the required energy to pre-condition outdoor air in winter and summer seasons. Due to the high ratio of heat transfer area to volume, Fixed-Bed Regenerators (FBRs) can reach high effectiveness up to 90%. However, limited research studies are available for FBRs in HVAC applications. In this paper, a small-scale test facility is used to determine the sensible effectiveness of a FBR. Furthermore, a numerical model is proposed and validated against the experimental results from the small-scale test facility. The numerical results for latent effectiveness have been compared with available data in the literature and the comparison shows a satisfactory agreement between numerical and results from the literature.

1 Introduction

The United Nations 17 sustainable development goals (SDGs) are a blueprint for creating a better and more sustainable world by 2030; these goals contain every challenge crucial to humanity's future. Goal 7 of SDGs aimed to ensure access to affordable, reliable, sustainable, and modern energy for all. Reliable and secure energy access has a dispensible role in achieving all SDGs [1].

The buildings and buildings' construction sector are responsible for around 33% of global final energy consumption, and around 40% of the total direct and indirect CO_2 emissions[2]. Population growth, urbanization, migration to larger cities and improvement of living standards, improving access to energy in developing countries, greater ownership and use of energy-consuming devices, and rapid growth in global buildings floor area are among the factors that result in the increasing energy demand for buildings and buildings construction sectos[2], [3]. The space heating and cooling of commercial, residential, and industrial buildings are responsible for 30-50% of energy consumption and greenhouse gas emissions in Canada[4] and EU[5]. Space heating, cooling, and ventilation of buildings are the main tasks of Heating, Ventilating, and Air Conditioning (HVAC) systems and account for 60% and 54% of the energy consumption by residential and commercial buildings, respectively[6]. Thus, It is estimated that HVAC systems make up 15-30% of global energy consumption[6].

Heating, ventilation, and air conditioning engineers and researchers are working on developing new technologies to reduce energy consumption while providing acceptable indoor air quality (IAQ) and thermal comfort prescribed by standards such as ASHRAE standard 62.2- 2019[7]. Indoor air quality and thermal comfort play a critical role in satisfaction, health, and productivity of occupants[8] who spend 90% of their time within built environments[9]. Indoor stale air is required to be replaced by the fresh outdoor air to maintain the prescribed level of indoor air quality, and this process is highly energy-intensive. Ambient parameters that affect thermal comfort include air temperature, relative humidity, airspeed, and radiant temperature. Depending on the season, building occupancy and activity level, temperature, and humidity should be maintained within specific ranges to meet the requirements of thermal comfort. Control of humidity is crucial to both comfort level and indoor air quality. Ineffective humidity control within the built environment increases indoor air pollutants such as mold, fungi, bacteria, and viruses that have adverse effects on occupants' health[10]. The standard practice of dehumidification in conventional HVAC systems requires cooling down the air temperature to the dew point temperature and reheating the airflow before introduction to the conditioned space; this cooling and overheating processes are ineffective and energy-intensive.

Incorporating an Air-to-Air Energy Exchangers (AAEEs) into HVAC systems is a well-recognized solution to increase energy efficiency through recover energy (heat and moisture) from the exhaust air and precondition (preheat or precool and humidify or dehumidify) the outdoor fresh air stream. Different types of energy recovery exchangers are available in the market, including fixed-plate exchangers, heat pipe, rotary exchanger (energy wheel), fixed-bed regenerators (FBRs), and run around membrane exchangers (RAMEE). AAEEs can be designed to recover only heat

* Corresponding author: hadi.ramin@usask.ca

(sensible) or simultaneous heat and moisture (total) from the exhaust airflow within HVAC systems.

AAEEs can also be categorized based on the way that heat and moisture exchange between two streams: regenerative and recuperative. Recuperative technologies are those which energy exchanges between two adjacent flows. However, in the case of regenerators, the two streams, periodically, flow in the same duct and energy stores and releases alternatively. There are two main types of regenerators, rotary (energy wheel) and stationary (fixed-bed) regenerators. Rotary regenerators have one rotating exchanger (a wheel), and fixed-bed regenerators (FBRs) have two stationary exchangers with dampers to alternate the airflow between them to maintain a continuous flow. If the exchanger surface of regenerators is coated with desiccants, they will be able to exchange both heat and moisture, while the surface without desiccant is able to exchange only heat between airflows. Rotary regenerators have been extensively studied in the literature[11]; however, studies regarding the application of stationary regenerators in HVAC systems in the literature are very limited[12]–[15], despite their promising effectiveness compare to other types of AAEEs.

Although several studies have been done to understand the physics of heat and moisture transfer in energy wheels, only a few studies have focused on the testing and modeling of fixed-bed heat and moisture regenerators for HVAC applications[11], [18], [19]. Nizotsev et al.[12], [20] performed experimental and numerical research on a heat exchanger mounted on the building wall with a reversible fan to create a periodic change in the airflow direction. They studied the variation of effectiveness with mass flow rate and air temperature. Chang et al.[21] developed a FBR using two stationary energy wheels and four fans. Hence, despite various applications of FBRs in furnaces and heat recovery systems in industries such as aluminum, cement and glass making, literature in the application of FBRs in HVAC systems are very limited[14], and thus the objectives of this study are to:

1. determine the sensible and latent effectiveness of FBR using small scale test facility, and
2. validate a numerical model for FBR in HVAC applications.

At this stage of the research, the sensible regenerator model results have been validated against the results from the experimental test setup. The experimental results for moisture transfer part (latent regenerator result) are not available at the time of submission of the paper and the results of the numerical model have been compared against the previous results published in the literature by Fathieh et al.[22].

2 Fixed-Bed Regenerator (FBR) operation and performance criteria

Figure 1 shows a schematic diagram of a FBR with two stationary exchangers, two fans, and dampers. To transfer energy between exhaust and supply air streams, the exchangers in Figure 1 undergo two phases of energy exchange. The operation of FBR during the winter season is explained as follows; the summer operation is similar while the heat and moisture exchange direction might reverse depending on the outdoor climate condition. For winter operation, in the first phase, the dampers are positioned as shown in Figure 1 (a) and the exhaust air (at 23°C and 50% RH) stream flows through EX1, and the supply air (-25°C and 70% RH, in Saskatoon winter for example) stream flows through EX2. The exhaust air heats and humidify EX1, while EX2 heats and humidify the supply air. In the second phase, all the dampers turn 90 degrees so that the flow through the exchangers is reversed (Figure 1(b)). The exhaust air flows through EX2, and the supply air flows through EX1. Thus the exhaust air heats and humidify EX2, while EX1 heats and humidify the supply air. This means that the energy is intermittently stored in the exchangers before it is transferred to the cold air stream. Therefore, the operation of each exchanger includes a heating and humidifying period (hot fluid flows through the exchanger) and a cooling and dehumidifying flow period (cold fluid flows through the exchanger). The duration of each phase is usually 60 seconds [16]. The exchanger channel is made up of heat and moisture storage material that allows heat and moisture exchange between the air streams.

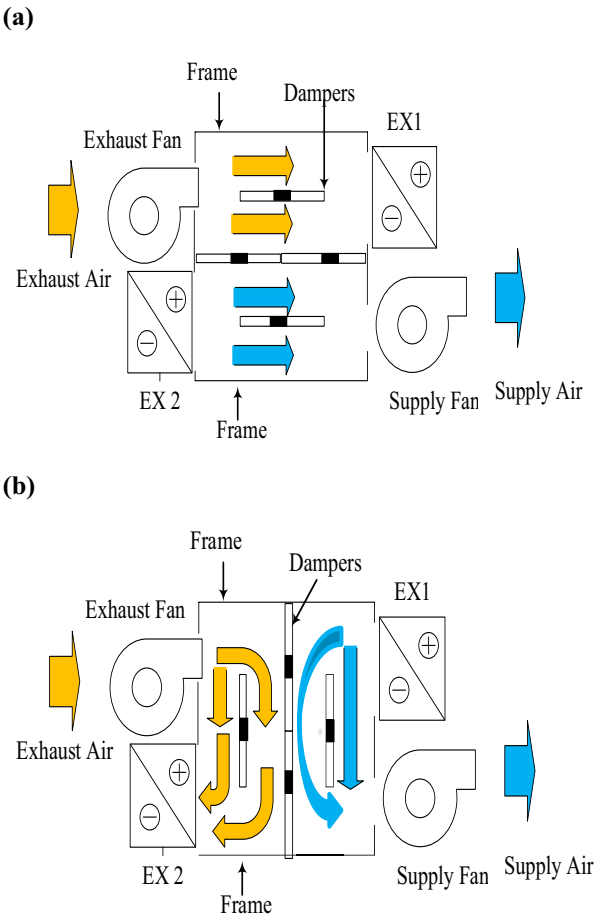

Figure 1. Schematic of operation of an FBR for energy recovery in buildings (a and b two phases of operation)

A FBR has a high transfer area per unit volume, can be easily integrated into the retrofit strategies and can be easily cleaned. Effectiveness is one of the significant parameters to quantify heat and moisture performance of exchangers. The heat transfer performance of an exchanger/regenerator is quantified using effectiveness. Sensible effectiveness, latent effectiveness, and total effectiveness are used to measure heat transfer, moisture transfer and enthalpy transfer of an energy exchanger respectively. The following equation is used to evaluate the effectiveness of the exchanger (FBR)[17]:

$$\epsilon_{s,l,t} = \frac{Actual\ transfer\ of\ moisture\ or\ energy}{Maximum\ possible\ transfer} = \frac{\dot{m}_{supply}(\bar{X}_{s,e} - X_{s,i})}{\min(\dot{m}_{supply}, \dot{m}_{exhaust})(X_{e,i} - X_{s,i})} = \frac{\dot{m}_{exhaust}(X_{e,i} - \bar{X}_{e,o})}{\min(\dot{m}_{supply}, \dot{m}_{exhaust})(X_{e,i} - X_{s,i})} \quad (1)$$

Where the effectiveness subscripts refer to sensible (ε_s), latent (ε_l) and total (ε_t) effectiveness. X can take temperature, humidity ratio, and enthalpy as the input to calculate corresponding effectiveness. $\dot{m}_{supply}$ and $\dot{m}_{exhaust}$ are supply and exhaust mass flowrates respectively. The inlet and outlet properties are designated with subscripts 'i' and 'e' for X in the above equation. Unlike recuperative exchangers, in FBR the outlet thermal properties (temperature, humidity ration and enthalpy) vary with time and hence the time-averaged value over the supply and exhaust period are used to calculate the effectiveness in equation 1; the time average outlet properties are denoted by $\bar{X}$ and is calculated using equation 2, as follows:

$$\bar{X}_{s,o} = \frac{1}{\tau_1}\int_0^{\tau_1} X_{s,o}dt \ \ and\ \bar{X}_{e,o} = \frac{1}{\tau_2}\int_0^{\tau_2} X_{e,o}dt \quad (2)$$

Where τ_1 and τ_2 are the duration in which the heat exchanger is exposed to the supply and exhaust airflow respectively.

3 Experimental test facility for sensible effectiveness

To determine the sensible effectiveness of FBRs a small-scale test facility is developed at the University of Saskatchewan as shown in Figure 2 (a). The experimental facility consists of air supply and a test section (see Figure 2 (b)). Two blowers are used to provide a continuous airflow to the test section. A parallel-plate exchanger (made of thin sheets of Aluminum 3003), as shown in Figure 2(c), is used in the test section. The small scale parallel-plate exchanger consists of 16 plates that form 15 flow channels; the airflow is equally distributed within the channels. The heat exchanger geometrical and thermophysical properties are presented in Table 1. The parallel plate exchanger is moved between the two air streams using a pneumatic controlled linear actuator. This periodical movement of the heat exchanger between hot and cold airflows represents the alternate heating and cooling of the heat exchanger within actual FBR. The flow rate to the test section is controlled by adjusting the voltage supplied to the blowers and the orifice plates measure the airflow rate on each supply line. One of the air streams is heated to 40°C (hot stream temperature) using a PID controlled duct heater (Omega AHF- 06120, 600 W) while the other stream is kept at room temperature of 24°C (cold stream temperature). The temperature of the hot and cold airstreams at the inlet and outlet of the exchanger are measured using calibrated T-type thermocouples with an uncertainty of ± 0.2°C.

4 Governing equations and numerical modeling

In FBR, the two separate air streams are alternatively fed into the heat exchanger which consists of numerous channels. Because of the similarity between the flow channels, the governing equations, assumptions and boundary conditions will be presented for a representing channel. The schematic of the cross-section of the representing channel is presented in Figure 3. In the first half cycle of operation, energy absorbs (solid lines in Figure 3) in the matrix and in the second half cycle, the energy releases from the matrix (dashed line in Figure 3).

The governing equations for the energy wheel presented by Simonson and Bestant[23], [24] are adopted in this paper for FBR since they are similar in terms of mathematical modeling. The conservation of mass in the air stream results in two continuity equations, for water vapor and dry air as follows:

$$A_g\frac{\partial \rho_v}{\partial t} + \frac{\partial}{\partial x}\left(\rho_v U A_g\right) + \dot{m}' = 0 \quad (3)$$

$$\frac{\partial \rho_a}{\partial t} + \frac{\partial}{\partial x}(\rho_a U) = 0 \quad (4)$$

Where U, $\dot{m}'$, A_g ρ_v and ρ_a are mean airflow velocity, rate of phase change per unit of length, the cross-sectional area of the channel, water vapor and dry air density, respectively. The conservation of mass for the desiccant is as follows:

$$\dot{m}' = \rho_{(d,dry)} A_d \frac{\partial u}{\partial t} \quad (5)$$

Where $\rho_{(d,dry)}$, A_d and u are the density of dry desiccant, the surface area of desiccant, and mass fraction of water in desiccant, respectively. The energy conservation equations for coupled heat and moisture transfer in regenerators for air stream and matrix are as follows:

$$\rho_g C_{P_g} A_g \frac{\partial T_g}{\partial t} + U\rho_g C_{P_g} A_g \frac{\partial T_g}{\partial x} - \dot{m}' h_{ad}\eta + h\frac{A_s'}{L}(T_g - T_m) = 0 \quad (6)$$

$$\rho_m C_{P_m} A_m \frac{\partial T_m}{\partial t} - \dot{m}' h_{ad}(1-\eta) - h\frac{A_s'}{L}(T_g - T_m) = \frac{\partial}{\partial x}\left(k_m A_m \frac{\partial T_m}{\partial x}\right) \quad (7)$$

Where t, x, C_p, k, h, L and T are time, axial coordinate, specific heat, thermal conductivity, convective heat transfer coefficient, length of channel and temperature, respectively. Subscripts 'g' and 'm' are used to represent the gas and matrix (desiccant and aluminum) variables, respectively. A'_s and A_m represent heat transfer surface area and cross-sectional area of the exchanger plate.

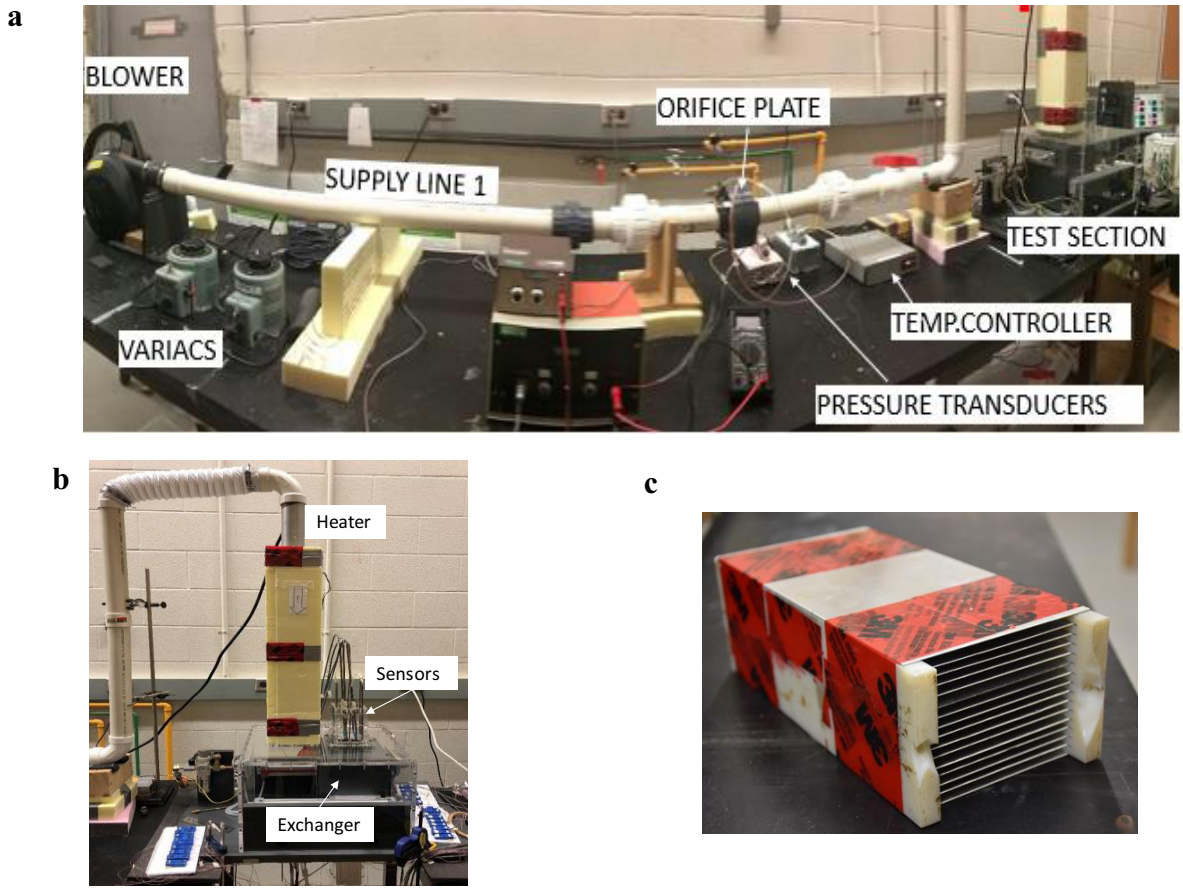

Figure 2: (a) Small scale test facility for the performance evaluation of FBRs, (b) a schematic of the test section and (c) a picture of the parallel-plate heat exchanger for the test section.

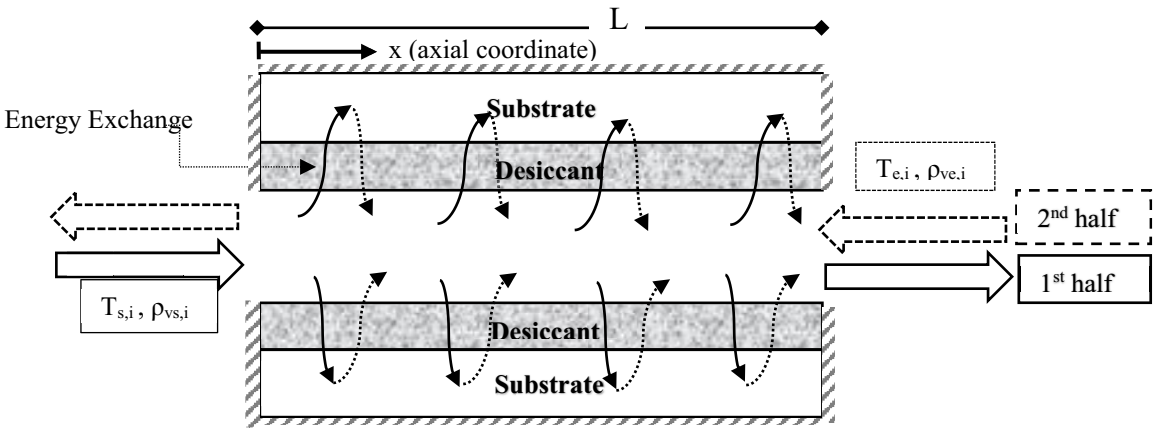

Figure 3: A schematic of the numerical domain for heat and mass transfer in the channel (solid line for the first half of the total cycle (exhaust flow in winter) and the dashed line for the second half of cycle (supply flow in winter)).

Table 1: Exchanger (channel and sheets) geometrical and thermophysical properties

Air channel				**Aluminum sheet**			
Width (cm)	Width (cm)	Height (mm)	Hydraulic diameter (mm)	Thickness (mm)	Density (kg/m^3)	Thermal Conductivity (W/m·K)	Specific heat capacity (J/kg·K)
20	8	4	7.6	0.62	2730	162	903

The term η in the above equations accounts for the distribution of phase change energy between the desiccant and the air. η can be determined as follows:

$$\eta = \frac{k_g/\sqrt{\alpha_g}}{k_g/\sqrt{\alpha_g} + k_m/\sqrt{\alpha_m}} \quad (8)$$

Where $\alpha_g$and α_m are thermal diffusivity of the airflow and matrix, respectively. Also, in the above equation $k_g = hD_h$.

Moisture transfer from the air stream to the matrix is one of the most important parts in this model, which can be obtained:

$$\dot{m}' = h_m \frac{A_s'}{L}(\rho_v - \rho_{v,m}) \quad (9)$$

Where h_m and $\rho_{v,m}$ are the convective mass transfer coefficient and water vapor density on the surface of desiccant respectively. $h_m$is determined using the analogy between heat and mass and $\rho_{v,m}$is obtained from the sorption isotherms.

Although the heat and mass transfer problem in regenerators is transient, its solution is periodic, therefore following periodicity conditions must be satisfied:

For the cold and dry side:

$$T_g(t,0) = T_{s,i}(t) \quad (10)$$
$$\rho_v(t,0) = \rho_{(v)_{s,i}}(t) \quad (11)$$

For the warm and humid side:

$$T_g(t,L) = T_{e,i}(t) \quad (12)$$
$$\rho_v(t,L) = \rho_{(v)_{e,i}}(t) \quad (13)$$

Furthermore, heat and mass transfer at the ends of the channel are negligible and the boundary conditions can be written as:

$$\left.\frac{\partial T_m}{\partial x}\right|_{x=0} = \left.\frac{\partial T_m}{\partial x}\right|_{x=L} = 0 \quad (14)$$

$$\left.\frac{\partial u}{\partial x}\right|_{x=0} = \left.\frac{\partial u}{\partial x}\right|_{x=L} = 0 \quad (15)$$

The transient transport equations for the conservation of energy in the airflow and matrix are discretized using a finite volume method. The upwind differencing and central differencing schemes are used to approximate the convection/diffusion terms in the airflow and the matrix, respectively. The resulting algebraic equation for the airflow is solved using a Gauss-Seidel iteration technique, and the Tridiagonal Matrix Algorithm (TDMA) is used to solve the energy equation in the matrix.

5 Results and Discussions

The results will be presented for two cases in this section: sensible and latent regenerator. For sensible regenerators, there is a temperature difference between two airstreams and the exchanger is made up of aluminum; desiccant is not coated on the surface of the plates in this case. Therefore, the temperature profile along with the sensible effectiveness from the current experimental test setup will be compared with the numerical results. For latent regenerator, the inlet temperatures of both airflows are equal, while there is a relative humidity difference between airflows. The current numerical results for outlet humidity ratio and latent effectiveness are compared with the experimental results by Fathieh et al.[22]. The sensible and latent results are presented in sections 5.1 and 5.2, respectively.

5.1. Sensible Regenerator

Figure 4 shows the experimental and numerical quasi-steady-state outlet air temperatures of the FBR at a face velocity of 1.2 (m/s) (volumetric flowrate is 350 (L/min)). The inlet air temperature on the hot side and the cold side are set to be 41°C and 24°C, respectively. The outlet temperature increases during the hot period and decreases during the cold period as expected. At the beginning of the hot and cold phases, the experimental measurements are considerably different from the numerical results. This deviation is mainly due to the slow response of the sensors during the transient (dynamic) temperature measurements. An analytical solution is obtained for the sensor response that is exposed to a temperature profile similar to that of FBR outlet, and the experimental data are modified accordingly to calculate effectiveness; this solution and further discussion are presented in a conference paper by the authors[25]. Except for this deviation, the numerical results and modified experimental results show a good agreement for the simulated range of operating conditions. The experimental results are modified to take into account the effect of delay in response of thermocouples for temperature measurements.

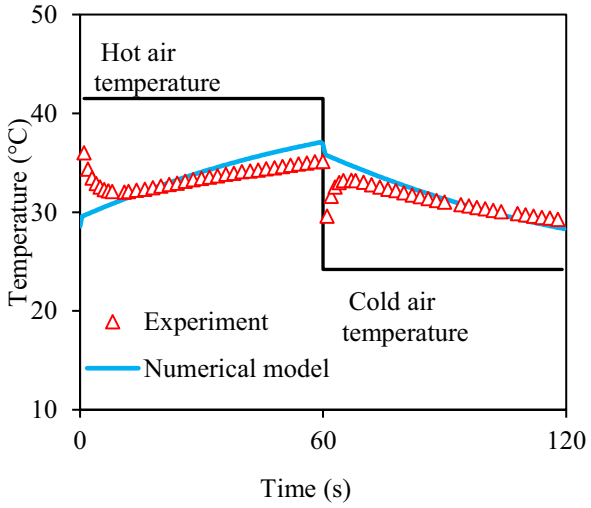

Figure 4. Experiment and numerical temperature profiles at the inlet and outlets of a FBR (face velocity: 1.2 m/s)

The sensible effectiveness of the FBR can be calculated from the periodic temperature profiles in Figure 4. From this Figure, the sensible effectiveness can

be obtained as the ratio of the actual heat transfer rate (the area between outlet temperature and hot air temperature in Figure 4) to the maximum possible heat transfer rate (the area between the hot side and cold side air temperature in Figure 4). The sensible effectiveness is obtained at the different cycle time and the numerical and experimental results are presented in Figure 5 along with the data from available correlation by Kay and London [26] in literature. Good agreement is also observed between the results and the prediction of the Kays and London[26] correlation.

5.2. Latent Regenerator

Moisture transfer occurs on the surface of parallel plates coated with desiccant material with a strong affinity for water vapor. Moisture is absorbed by the desiccant particle when the humid air passes through the desiccant coated channel, while during the exposure of the exchanger to dry air stream, the accumulated water vapor on the surface of desiccant transfers to the airflow. The sorption properties of desiccant material play a major role in the water vapor transfer rate. Water vapor partial pressure or relative humidity in the air streams acts asdriving force for moisture transfer rate. Equilibrium sorption isotherm for the desiccant material (in this case silica gel) is used to obtain the relative humidity of water vapor at the desiccant surface. The water vapor adsorption isotherm for the silica gel sample is adopted from [22] and is shown in Figure 6. Properties of silica gel and operating conditions for the latent regenerator are presented in Table 2. The aluminum properties and geometrical details are the same as in Table 1.

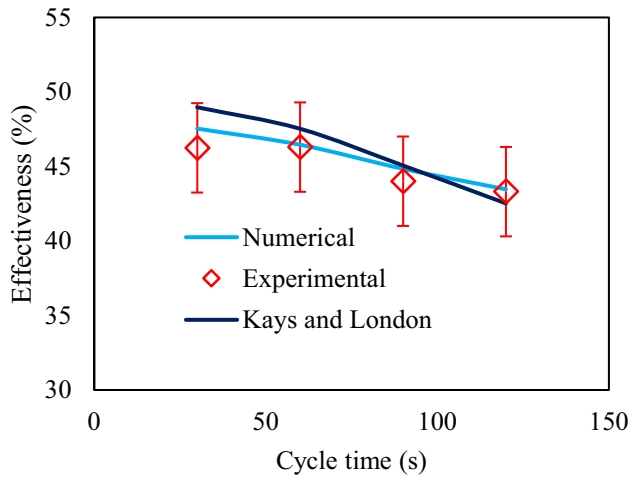

Figure 5. Comparison of sensible effectiveness obtained from the experiments, numerical model and design correlation at different cycle times

Normalized humidity is defined as:

$$W(t) = \frac{W_{out} - W_{inlet,dry}}{W_{inlet,humid} - W_{inlet,dry}} \quad (16)$$

Where W is the humidity ratio of the airflow.

The quasi-steady-state normalized humidity is obtained from the numerical simulation for the total cycle time of 120 seconds and this profile is presented in Figure 7 along with the experimental results presented by Fatheih et al. [22]. The normalized humidity is given for four cycles of 120 seconds (total 480 seconds) in Figure 7. The comparison between numerical and experimental results in this figure indicates a good agreement between the results.

The latent effectiveness of the FBR is obtained from the humidity profile and equation (1). The latent effectiveness for the total cycle time of 120 seconds is equal to 33.5%, which agrees with the experimental data (29±5%) from Fatheih et al. [22] within the experimental uncertainty range.

Table 2. Silica gel (SG) properties[27] and the test operating condition from[22]

Description	value
Density of SG (kg/m3)	615
Specific heat capacity of SG (J/kg·K)	476
The fraction of phase change energy convected to the air is (η)	0.05
Inlet dry and humid temperature (°C)	24.0
RH of dry air (%)	5
RH of humid air (%)	50
Total cycle time (s)	120
Volumetric flow rate (L/min)	100
Mean airflow velocity (m/s)	0.34
Reynolds number	174

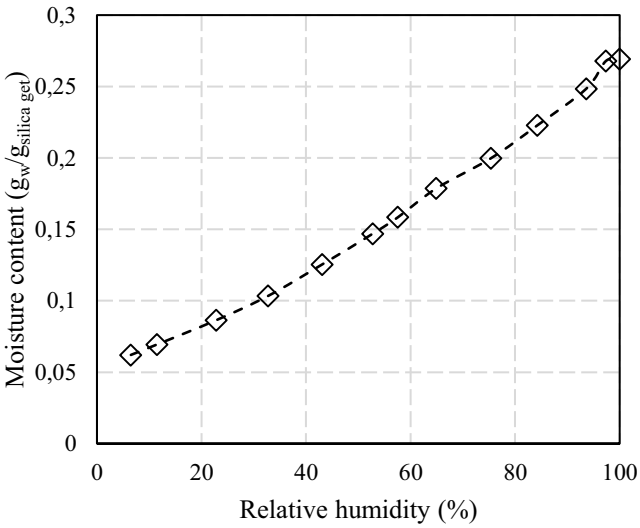

Figure 6. Adsorption isotherm of water vapor on the mesoporous silica gel at 23°C [22]

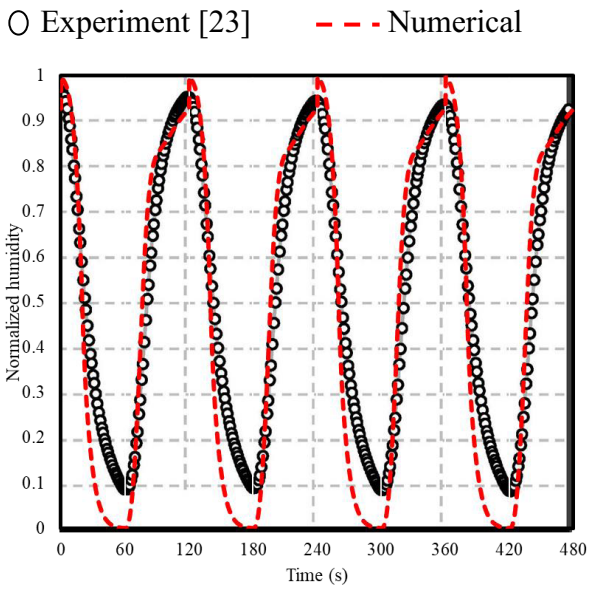

Figure 7. Quasi-steady state normalized humidity from the numerical simulation and experimental results of Fathieh et al.[22] at a total cycle time of 120 seconds and flow rate: 100 L/min

6 Conclusions

This paper uses a small-scale experimental facility and a numerical model to determine the sensible effectiveness of fixed-bed regenerators (FBRs) for HVAC applications. The numerical and experimental results for sensible effectiveness agrees within the uncertainty range of experimental results. The importance of transient measurement of temperature for FBR is discussed and the experimental results were modified to include this effect.

The outlet humidity profile of FBRs is obtained from the numerical model and the results were in a satisfactory agreement with the previous data published in the literature. However, further study and experimental data are required to understand the moisture transfer process in FBRs, especially the transient response of humidity sensors within FBRs would be the topic of future studies.

Future works will use the model and experimental facility to optimize FBRs for simultaneous heat and moisture transfer.

Financial support from the College of Engineering and Postdoctoral Studies of the University of Saskatchewan, National Science and Engineering Research Council (NSERC) and Tempeff North America Inc., Winnipeg are appreciated.

References

[1] "Goal 7: Sustainable Development Knowledge Platform." [Online]. Available: https://sustainabledevelopment.un.org/sdg7. [Accessed: 02-Jan-2020].

[2] "Buildings – Topics - IEA." [Online]. Available: https://www.iea.org/topics/buildings. [Accessed: 05-Jan-2020].

[3] H. Ramin, P. Hanafizadeh, T. Ehterami, and M. A. AkhavanBehabadi, "Life cycle-based multi-objective optimization of wall structures in climate of Tehran," *Adv. Build. Energy Res.*, vol. 13, no. 1, pp. 18–31, 2019.

[4] NRCan, "Energy Efficiency Trends in Canada 1990-2010," Natural Resources Canada, 2010.

[5] E. Union, "Heating and cooling | Energy." [Online]. Available: https://ec.europa.eu/energy/en/topics/energy-efficiency/heating-and-cooling. [Accessed: 05-Jan-2020].

[6] M. Shakouri, E. N. Krishnan, A. H. Karoyo, L. Dehabadi, L. D. Wilson, and C. J. Simonson, "Water Vapor Adsorption-Desorption Behavior of Surfactant-Coated Starch Particles for Commercial Energy Wheels," *ACS Omega*, vol. 4, pp. 14378–14389, 2019.

[7] ASHRAE, *ANSI/ASHRAE Standard 62.2-2019: Ventilation and acceptable indoor air quality in residential buildings*. Atlanta: ASHRAE, 2019.

[8] F. Mofidi and H. Akbari, "Personalized energy costs and productivity optimization in offices," *Energy Build.*, vol. 143, pp. 173–190, 2017.

[9] C. Schweizer *et al.*, "Indoor time-microenvironment-activity patterns in seven regions of Europe," *J. Expo. Sci. Environ. Epidemiol.*, vol. 17, no. 2, pp. 170–181, 2007.

[10] A. V. Arundel, E. M. Sterling, J. H. Biggin, and T. D. Sterling, "Indirect health effects of relative humidity in indoor environments," *Environ. Health Perspect.*, vol. VOL. 65, no. 3, pp. 351–361, 1986.

[11] C. J. Simonson and R. W. Besant, "Energy wheel effectiveness: Part I-development of dimensionless groups," *Int. J. Heat Mass Transf.*, vol. 42, no. 12, pp. 2161–2170, 1999.

[12] M. I. Nizovtsev, V. Y. Borodulin, V. N. Letushko, and A. A. Zakharov, "Analysis of the efficiency of air-to-air heat exchanger with a periodic change in the flow direction," *Appl. Therm. Eng.*, vol. 93, pp. 113–121, 2016.

[13] C. C. Chang, J. De Liang, and S. L. Chen, "Performance investigation of regenerative total heat exchanger with periodic flow," *Appl. Therm. Eng.*, vol. 130, pp. 1319–1327, 2018.

[14] H. Ramin, E. N. Krishnan, and C. J. Simonson, "Fixed bed regenerators for HVAC applications," *27th Can. Congr. Appl. Mech.*, pp. 1–6, 2019.

[15] E. Krishnan, H. Ramin, and C. J. Simonson, "performance testing of fixed-bed regenerators for hvac," in *The Second Pacific Rim Thermal Engineering Conference*, 2019, pp. 1–5.

[16] "Heat Recovery System | Heat Recovery Ventilator | ERV | Energy Recovery." [Online]. Available: https://www.tempeffnorthamerica.com/. [Accessed: 12-Jul-2019].

[17] ASHRAE, *Method of Testing Air-to-Air Heat/Energy Exchangers, ASHRAE 84-2013*. Atlanta, 2014.

[18] L. A. Sphaier and W. M. Worek, “Analysis of heat and mass transfer in porous sorbents used in rotary regenerators,” *Int. J. Heat Mass Transf.*, vol. 47, no. 47, pp. 3415–3430, 2004.

[19] C. J. Simonson and R. W. Besant, “Energy wheel effectiveness : part II part -correlations,” *Int. J. Heat Mass Transf.*, vol. 42, pp. 2171–2185, 1999.

[20] M. I. Nizovtsev, V. Y. Borodulin, and V. N. Letushko, “Influence of condensation on the efficiency of regenerative heat exchanger for ventilation,” *Appl. Therm. Eng.*, vol. 111, pp. 997–1007, 2017.

[21] C. C. Chang, C. H. Lai, C. M. Yang, Y. C. Chiang, and S. L. Chen, “Thermal performance enhancement of a periodic total heat exchanger using energy-storage material,” *Energy Build.*, vol. 67, pp. 579–586, 2013.

[22] F. Fathieh *et al.*, “Determination of air-to-air energy wheels latent effectiveness using humidity step test data,” *Int. J. Heat Mass Transf.*, vol. 103, pp. 501–515, 2016.

[23] C. J. Simonson and R. W. Besant, “Energy wheel effectiveness: part II-correlations,” *Int. J. Heat Mass Transf.*, vol. 42, pp. 2171–2185, 1999.

[24] C. J. Simonson and R. W. Besant, “Energy wheel effectiveness: Part I-development of dimensionless groups,” *Int. J. Heat Mass Transf.*, vol. 42, no. 12, pp. 2161–2170, 1999.

[25] H. Ramin, E. N. Krishnan, W. Alabi, and C. J. Simonson, “Temperature Measurement Correction for the Determination of the Effectiveness of Fixed-Bed Regenerators (FBRs) for HVAC Applications,” in *2020 ASHRAE winter conference*, 2020.

[26] W. M. Kays and A. L. London, *Compact Heat Exchangers*, Third edit. New York: McGraw-Hill, Inc, 1984.

[27] C. J. Simonson and R. W. Besant, “Heat and Moisture Transfer in Desiccant Coated Rotary Energy Exchangers : Part I Numerical Model,” *HVAC&R Res.*, vol. 3, no. 4, pp. 325–350, 1997.